DISCRETE AND CONTINUOUS
DYNAMICAL SYSTEMS

doi:10.3934/dcds.2021075

THE GRAPH OF THE LOGISTIC MAP IS A TOWER

Roberto De Leo*

Department of Mathematics
Howard University
Washington, DC 20059, USA

James A. Yorke

Institute for Physical Science and Technology and the Departments of Mathematics and Physics
University of Maryland
College Park, MD 20742, USA

(Communicated by Enrico Valdinoci)

In memory of Todd A. Drumm (1961-2020) and Tien-Yien Li (1945-2020).

Abstract. The qualitative behavior of a dynamical system can be encoded in a graph. Each node of the graph is an equivalence class of chain-recurrent points and there is an edge from node A to node B if, using arbitrary small perturbations, a trajectory starting from any point of A can be steered to any point of B. In this article we describe the graph of the logistic map. Our main result is that the graph is always a tower, namely there is an edge connecting each pair of distinct nodes. Notice that these graphs never contain cycles. If there is an edge from node A to node B, the unstable manifold of some periodic orbit in A contains points that eventually map onto B. For special parameter values, this tower has infinitely many nodes.

1. **Introduction.** Ever since H. Poincaré invigorated the field of qualitative Dynamical Systems in late 1800s, one of its main goals has been understanding the qualitative asymptotic behavior of points under a continuous or discrete time evolution. In this article we study some fundamental qualitative aspect of the dynamics of the logistic map $\ell_\mu(x) = \mu x(1-x)$ and we represent our results into a graph.

The idea of describing the asymptotics of points in a dynamical system through a graph goes back at least to S. Smale. In Sixites, he observed [34, 35] that, as a byproduct of Morse theory, the flow of the gradient vector field of a Morse function f on a compact manifold M can be encoded into a graph: 1. Its non-wandering set $\Omega_f \subset M$ consists in just a finite number of fixed points Ω_i, $i = 0, \dots, p$; these are the nodes of the graph. 2. The dynamics outside Ω_f consists just of orbits asymptotic

2020 *Mathematics Subject Classification.* 26A18, 37B20, 37B35, 37E05.

Key words and phrases. Logistic map, chain-recurrent sets, graph of a dynamical system, towers, spectral theorem.

This material is based upon work partially supported by the National Science Foundation under Grant No. 1832126.

* Corresponding author: Roberto De Leo.

to a fixed point Ω_i for $t \to \infty$ and a different fixed point Ω_j for $t \to -\infty$; in this case, we say that there is an edge from Ω_j to Ω_i.

Smale also showed that this idea also applies to the more general case of *Axiom-A* diffeomorphisms on compact manifolds if we just replace *fixed points* with *closed disjoint invariant indecomposable subsets* Ω_i, on each of which f is topologically transitive. Recall that, for a Axiom-A diffeomorphism f, the non-wandering set Ω_f is hyperbolic and the set of periodic points is dense in it. In this case, the nodes of the graph are the Ω_i and there is an edge from Ω_i to Ω_j if and only if the intersection of the stable manifold of Ω_i with the unstable manifold of Ω_j is non-empty. Important examples of Axiom-A diffeomorphisms are Morse-Smale diffeomorphisms (those whose nonwandering set consists in a finite number of hyperbolic periodic orbits) and Anosov diffeomorphisms (those for which the whole manifold is hyperbolic).

Charles Conley extended this idea so that it can be applied to any kind of discrete or continuous dynamical system [9]. One of his key ideas was replacing the non-wandering set by the larger set of chain-recurrent points. Chain-recurrent points can be sorted into closed disjoint invariant sets N_i and Conley was able to prove that the dynamics outside of the N_i is gradient-like, namely every trajectory of points outside the chain-recurrent set represents an edge from some N_i to some N_j.

The first to study the non-wandering set of the logistic map were possibly Smale and Williams [36]. They studied the particular case $\mu = 3.83$, in which case there is a period-3 orbit attractor, and showed that the non-wandering set is given by the union of the attractor, the fixed repelling point 0 and a Cantor set on which the map acts as a subshift of finite type. This invariant Cantor set is topologically invariant for μ in the period-3 window (in Figs. 1 and 2 we show that set painted in red). A few years later, a complete description of the structure of the non-wandering set was given by Jonker and Rand for unimodal maps [23] and by van Strien for S-unimodal maps [37], which includes the case of the logistic map.

Although the structure of the non-wandering set has been known for forty years, no one so far has described the graph of the logistic map. The main goal of this article is to provide such a description. We achieve this by first studying the structure of the chain-recurrent set of the logistic map ℓ_μ. Each node N has a periodic point $p_1(N)$ that is closest point of the node to the critical point $c = 0.5$. We denote by $\rho(N)$ that minimum distance and say that nodes that have larger $\rho(N)$ values are "higher" than nodes with lower values. We denote by $J_1(N)$ the interval whose endpoints are $p_1(N)$ and $q_1 = 1 - p_1(N)$ and show that $J_1(N)$ maps into itself under some positive power k of ℓ_μ. This interval $J_1(N)$ is the first one of a cycle of intervals $\mathcal{T}(N) = \{J_1(N), \ell_\mu(J_1(N)), \ldots, \ell_\mu^{k-1}(J_1(N))\}$, invariant under ℓ_μ and containing the attractor. We call $\mathcal{T}$ a "cyclic trapping region". Some example of the intervals J_1 associated to different nodes are shown in Figs. 3 and 4.

Each cyclic trapping region $\mathcal{T}$ is accompanied by two structures: (1) the periodic orbit of the point p_1; (2) the node N containing p_1. Notice that no points of N are in the interior of the trapping region. Using the pairing between trapping regions and nodes, we ultimately show that there is an edge of the graph between each pair of nodes, from the higher to the lower.

We call such a graph a tower. The node at the bottom of a tower is attracting, all other ones are repelling. In a tower, arbitrarily close to each node N, for each lower node N', there are points falling eventually on N'. There are values of μ for which the tower has infinitely many levels. Examples of tower graphs of the logistic map

are shown in Fig. 1 and 2. In a follow-up paper [10] we present numerical evidence that infinite towers appear also as part of bifurcation diagrams of dissipative systems in higher dimension, such as the Poincaré return map of the Lorenz system.

The paper is structured as follows. All our results are contained in Sec. 3.2 and the reader is recommended to start reading the article from there and to use the rest as needed. In order to keep the article self-consistent we include in Sec. 2, all definitions and properties we use about chain-recurrence and the graph of a dynamical system and, in Sec. 3.1, the main theorems in literature we use to prove our own results of Sec. 3.2.

2. Chain-recurrence and the graph.

Throughout this paper, by dynamical system we mean a continuous map $\Phi : X \to X$ on a compact metric space (X, d). The orbit of a point $x \in X$ under Φ is the set $\{x, \Phi(x), \Phi^2(x), \dots\}$, where

$$\Phi^n = \underbrace{\Phi \circ \cdots \circ \Phi}_{n \text{ times}}.$$

In this article, we discuss extensively two classes of points, which we define below: non-wandering points and chain-recurrent points.

Definition of non-wandering point. A point $x \in X$ is a **non-wandering point** for Φ if, for every neighborhood U of x, there is a $n \geq 1$ such that $U \cap \Phi^n(U) \neq \emptyset$. We denote by Ω_Φ the set of all non-wandering points of Φ.

Notice that every point of a period-k orbit, that is, every fixed point of Φ^k, is trivially a non-wandering point.

Definition of chain-recurrence. Given two points $p, q \in X$ and an $\varepsilon > 0$, we say that there is a **ε-chain** [5] from p to q if there is a finite sequence of points $p = x_0, x_1, \dots, x_n = q$ on X such that, for $i = 0, \dots, n-1$,

$$d(\Phi(x_i), x_{i+i}) \leq \varepsilon. \tag{1}$$

We say that **q is downstream from p** if, for every $\varepsilon > 0$, there is a ε-chain from p to q; equivalently, we say that **p is upstream from q**. We write **$p \sim q$** if p is upstream and downstream from q, and we say that **p is chain recurrent** if $p \sim p$.

We denote by **$\mathcal{R}_\Phi$** the **chain-recurrent set** [9], *i.e.* the set of all chain-recurrent points of Φ. We call each equivalence class in $\mathcal{R}_\Phi$ a **node**. Hence, if x is in a node N, then $y \in N$ if and only if $x \sim y$.

If a point is non-wandering, it is certainly chain-recurrent. However, the following example shows that not all chain-recurrent points are non-wandering.

Let Ψ map $[0, 2\pi]$ into itself such that $\Psi(0) = 0$; $\Psi(2\pi) = 2\pi$; and $\alpha < \Psi(\alpha) < 2\pi$ for $\alpha \in (0, 2\pi)$. We identify 0 with 2π to make Ψ a map from the circle to itself. Then $\lim_{k\to\infty} \Psi^k(\alpha) = 0$ for all angles α and $\Omega_\Psi = \{0\}$.

In contrast, $\mathcal{R}_\Psi$ is the whole circle and so it is strictly larger than Ω_Ψ. Indeed, notice that every point α_0 of the circle converges under Ψ to 0 both forward and backwards. Hence, for every $\varepsilon > 0$, there is a piece of a trajectory $x_0, \dots, x_n$ such that $x_0 \in (0, \varepsilon/2)$, $x_i = \alpha_0$ for some $0 \leq i \leq n$ and $x_n \in (2\pi - \varepsilon/2, 2\pi)$. Then, $x_i, x_{i+1}, \dots, x_n, x_0, \dots, x_{i-1}, x_i$ is a ε-chain from α_0 to itself, *i.e.* every point of the circle is chain-recurrent.

Definitions of trajectories. For a map Φ, we will say that the bi-infinite sequence p_n, $n \in \mathbb{Z}$, is a **trajectory** if $p_{n+1} = \Phi(p_n)$ for all $n \in \mathbb{Z}$. Its forward (resp. backward) limit set **$\omega(t)$** (resp. **$\alpha(t)$**) is the set of the accumulation points of the

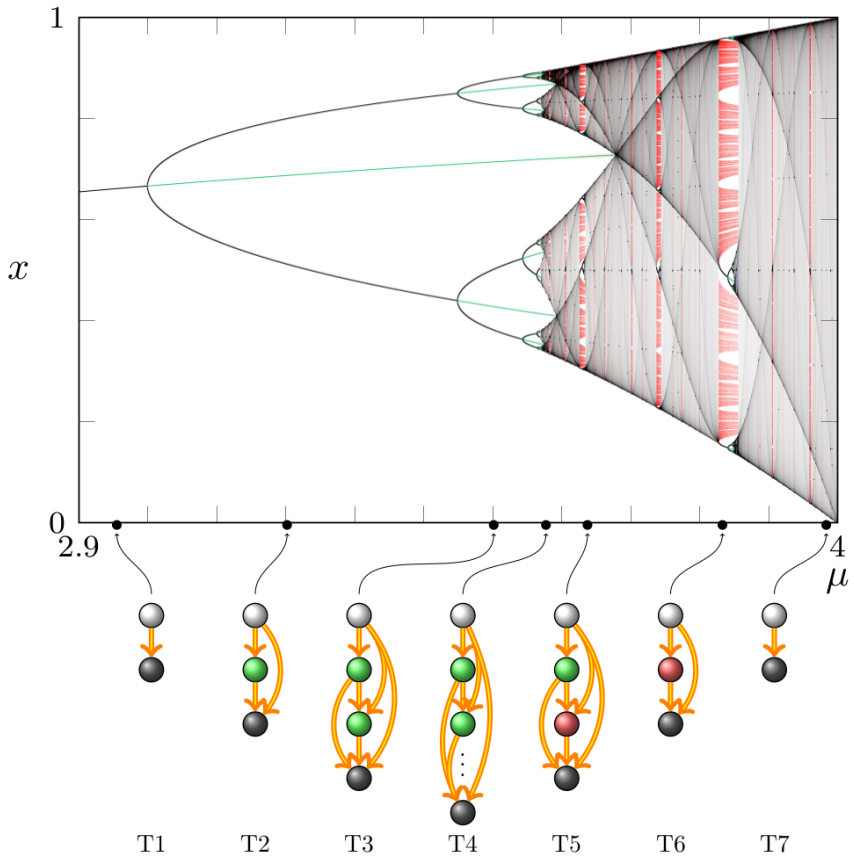

FIGURE 1. **Bifurcations diagram and sample graphs of the logistic map.** For each value of μ, the attracting set is painted in shades of gray, depending on the density of the attractor, repelling periodic orbits in green, and repelling Cantor sets in red. The "black dots" that are visible within the diagram are low-period periodic points. They signal the presence of bifurcation cascades within some window. The fact that some of them keep close to the line $x = c$ is a reflection of Singer's Theorem: when the attractor is a periodic orbit, c belongs to its immediate basin. For selected values of μ we also show, below the diagram, the graph of the corresponding logistic map.

trajectory for $n \to \infty$ (resp. $n \to -\infty$). For some maps, the inverse is not unique. For the map $z \mapsto z^2$, each point other than 0 has two inverses. Hence there will be infinitely many trajectories through a given $p_0 \neq 0$. Two different trajectories through p_0 will have the same forward limit set but might have different backward limit sets.

Proposition 1. *For every trajectory t, either the trajectory lies entirely in a node or there are two distinct nodes N_1, N_2 such that $\alpha(t) \subset N_1$ and $\omega(t) \subset N_2$.*

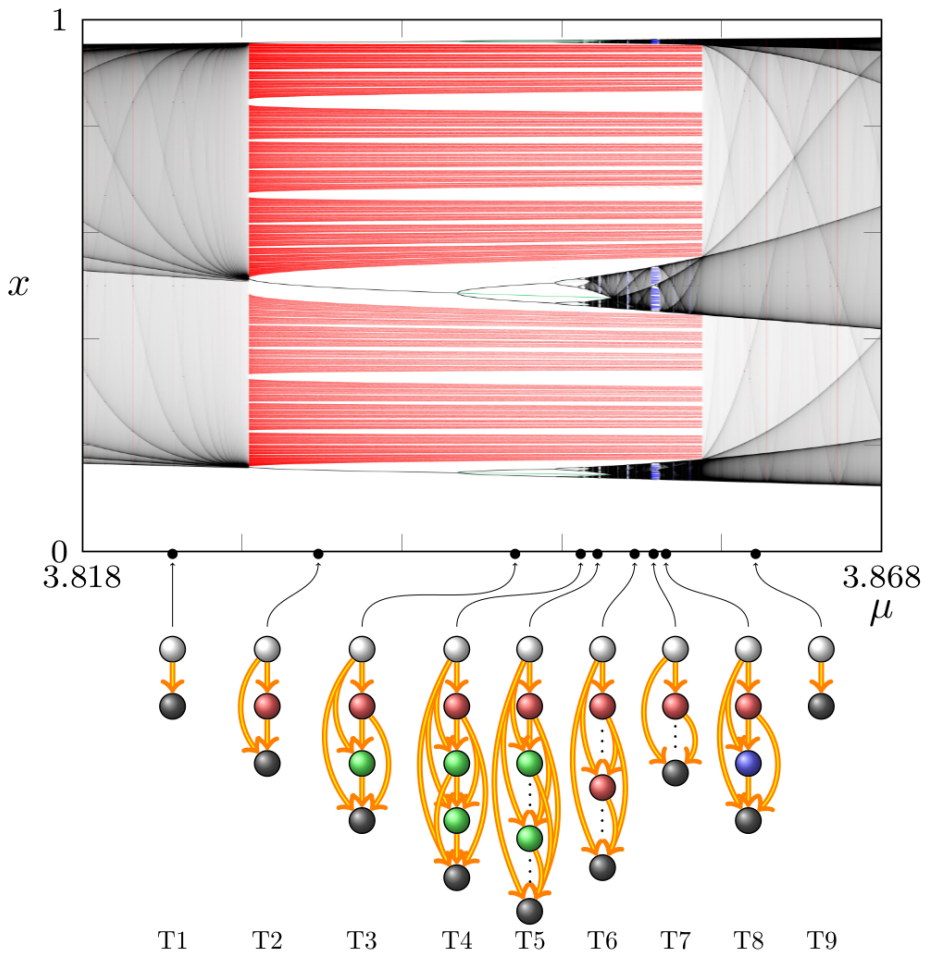

FIGURE 2. **Towers of nodes in the period-3 window of the logistic map.** The period-3 window W starts at $\mu \simeq 3.8284$ and ends at $\mu \simeq 3.8568$. At every μ within W, an invariant Cantor set node N (in red in figure) arises, depending continuously on μ. This is exactly the Cantor set discussed by Smale and Williams in [36] at $\mu = 3.83$. The widest white interval within the Cantor set is the $J_1(N)$ interval of the period-3 trapping region $\mathcal{T}(N)$ running throughout W. The periodic endpoint $p_1(N)$ of $J_1(N)$ is the top endpoint, the bottom one is $q_1 = 1 - p_1(N)$. The blue Cantor set node N' visible in figure is the node of a regular trapping region $\mathcal{T}(N')$ nested in $\mathcal{T}(N)$. As in Fig. 1, below the diagram we show the graph of the logistic map for selected values of μ.

Definition of attractor. Assume X is a measure space. Following Milnor [27], we say that a closed invariant set A is an **attractor** if it satisfies the following conditions:

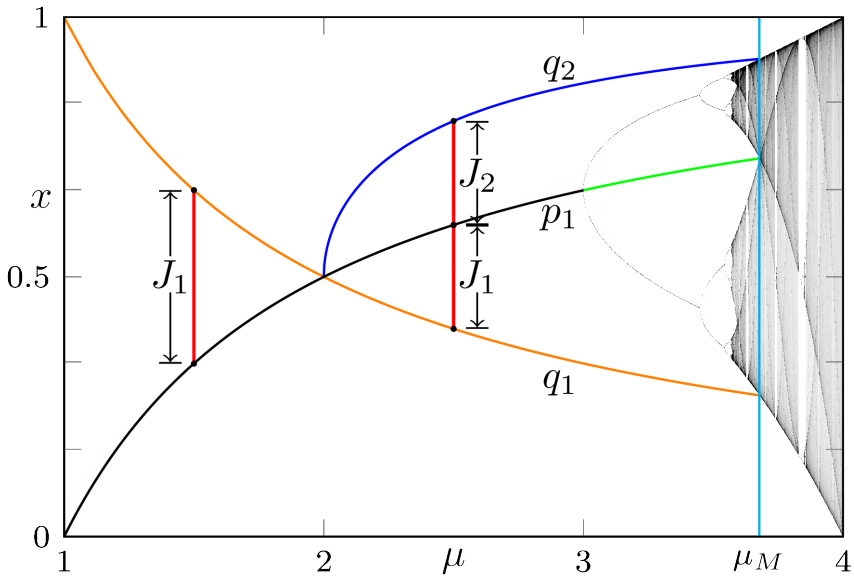

FIGURE 3. **Flip and regular trapping regions associated to a periodic orbit node.** The fixed point p_1 is a node for $1 < \mu < \mu_M$ (see Eq. 3). Each node has its own p_1, q_1 and J_1. It is attracting for $\mu < 3$. For $\mu < 2$, the trapping region associated with it consists of a single interval $J_1 = [p_1, q_1]$, where $q_1 = 1 - p_1$. As μ increases past the super-stable value $\mu = 2$, the trapping region becomes flip and consists of two intervals $J_1 = [q_1, p_1]$ and $J_2 = [p_1, q_2]$, with $\ell_\mu(q_2) = q_1$. The flip trapping region ends when p_1 hits the chaotic attractor at μ_M (Eq. 3). The region $3.4 \leq \mu \leq 3.6$ is shown in greater detail in Fig. 6.

1. the basin of attraction of A, namely the set of all $x \in X$ such that $\omega(x) \subset A$, has strictly positive measure;
2. there is no strictly smaller invariant closed subset $A' \subset A$ whose basin differs from the basin of A by just a zero-measure set.

We call a node an **attracting node** if it contains an attractor, otherwise we call it a **repelling node**.

This definition of attractor is more appropriate for the logistic map than the more common definition that an attractor must attractor all points in some neighborhood.

For instance, The logistic map has a countable number of parameter values for which there is an attractor-repellor bifurcation at which a pair of periodic orbits is created. At such points, the periodic orbit is attracting from one side and repelling from the other side. Hence it is an attractor by our choice of definition. Notice, moreover, that such an attractor-repellor orbit is a subset of an invariant Cantor set. We will show that this Cantor set is a node. Hence, by Milnor's definition, the node is an attracting node even though only part of it attracts.

Similarly, there are parameter values where there are windows within windows infinitely deep, yielding a node which attracts almost every trajectory but whose

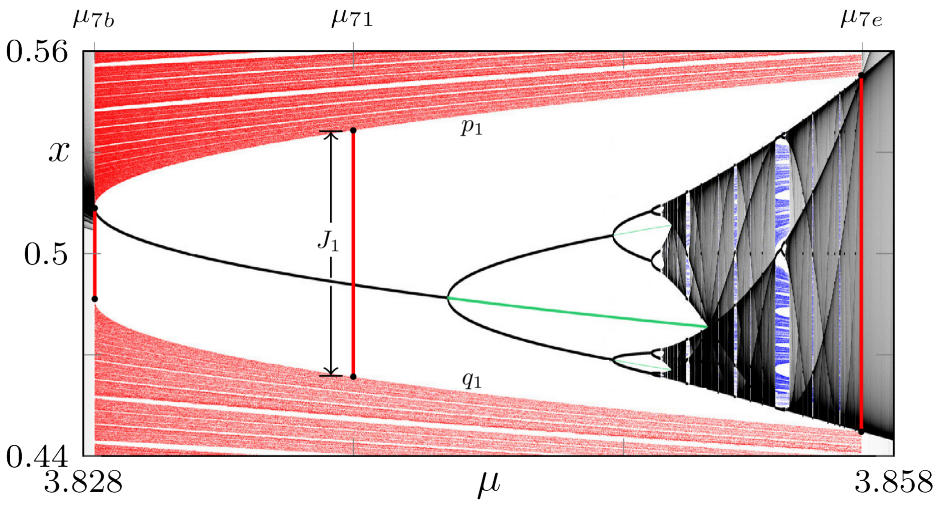

FIGURE 4. **A trapping region associated to a Cantor set node.** This window is a blowup of a region in Fig. 2. The red region is a Cantor set (for each μ in the window). The Cantor set is a node. The interval $J_1 = [q_1, p_1]$ is a trapping region of ℓ_μ^3 for each μ in the window. Each node has a trapping region for ℓ_μ and J_1 is the piece of the trapping region that contains the critical point. For each μ in the interior of the window, the point p_1 belongs to a repelling period-3 orbit within the red Cantor set and $\ell_\mu(q_1) = p_1$. There is a μ Within J_1 arises a bifurcation diagram qualitatively identical to the full one. The Cantor set node in blue within the period-3 window of the diagram inside J_1 is the analog of the red Cantor set within the main period-3 window. Fig. 7 shows the same region but with more detail.

basin does not contain an open set. Nonetheless, it is an attractor in the Milnor sense.

The graph. Conley [8, 9] realized that chain-recurrence could be used to define a graph of a dynamical system. His investigations concerned dynamical systems that come from ordinary differential equations on compact spaces but, over the years, his results have been extended to several other settings; in particular: continuous maps [28], semi-flows [31, 19, 30], non-compact [21, 30] and even infinite-dimensional spaces [31, 26, 7, 18] (notice that, throughout this article, we sort multiple citations in the order of their year of publication).

Definition of Liapunov function. A **Lyapunov function** [38, 28] for $\Phi : X \to X$ is a continuous function L such that:

1. L is constant on each node;
2. L assumes different values on different nodes;
3. $L(\Phi(x)) < L(x)$ if and only if x is not chain-recurrent.

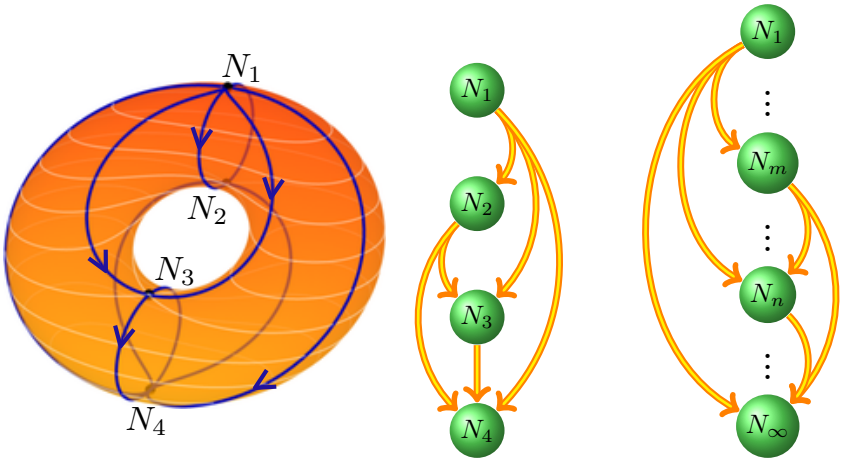

FIGURE 5. **An example of graph. (LEFT)** Dynamics induced on the 2-torus by the gradient vector field of the height function. In this case the Lyapunov function is the height function itself, some level set of which is shaded in white. In blue are shown the heteroclinic trajectories joining the critical point (which are exactly the invariant sets of this dynamical system). **(CENTER)** The graph of the dynamical system on the left. In this case it is a 4-levels tower. (RIGHT) An infinite tower.

Discrete Conley Theorem 1 (Norton, 1995 [29])**.** Let Φ be a dynamical system on a compact metric space X. Then there is a Lyapunov function for Φ.

The Discrete Conley Theorem allows to associate a graph to any dynamical system as follows.

Definition of graph of a dynamical system. The **graph** Γ of a dynamical system $\Phi : X \to X$ is a directed graph whose nodes are the nodes of Φ. Γ has an edge from node N to node N' if and only if there exist a trajectory t of Φ with $\alpha(t) \subset N$ and $\omega(t) \subset N'$.

The graph of a dynamical system has no loops. Notice that from the Discrete Conley Theorem it follows that, if there is an edge from N to N', there cannot be an edge from N' to N. Moreover, there cannot be any loops, that is, there cannot be a collection of nodes $N_1, \ldots, N_k$ such that there is an edge from N_i to N_{i+1}, for $i = 1, \ldots, k-1$, and from N_k to N_1.

Definition of tower. We say that a graph Γ is a **tower** if there is an edge between every pair of distinct nodes of Γ.

Towers are the kind of graph that this article is about. We show in Fig. 5 some example of tower with finitely and infinitely many nodes. Since we assume X to be compact, in a tower there is always a lowest node and it contains a Milnor attractor. An elementary example of dynamics with such a graph is the gradient flow of a Morse function on the 2-torus (see Fig. 5, right).

3. **The logistic map.** The logistic map

$$\ell_\mu(x) = \mu x(1-x),\ x \in [0,1],\ \mu \in [0,4], \tag{2}$$

is among the simplest continuous maps giving rise to a non-trivial dynamics. We recall that a continuous map $f : [0,1] \to [0,1]$ with $f(0) = f(1) = 0$ and for which there is a point $c \in (0,1)$ such that f is strictly increasing (resp. decreasing) for $x < c$ and strictly decreasing (resp. increasing) for $x > c$, is called **unimodal**. Moreover, a unimodal map f is **S-unimodal** if it is at least C^3 and its Schwarzian derivative (see [33]) is negative for every $x \neq c$. Notice that the logistic map is a S-unimodal map.

For $\mu \in (0,1]$, the point 0 is the unique attractor of ℓ_μ and its basin of attraction is the whole segment $[0,1]$. From now on, we will assume that $\mu \in (1,4]$.

The focus of the present work is on the edges in the graph of the logistic map. Indeed, as we will discuss below, while the structure of the invariant attracting and repelling sets have been thoroughly studied at several levels of generality, no one seems to have focused on the edges of the graph for the logistic map. Hence we do.

We have written this section so that the reader will gain a detailed picture of the possible chain-recurrent sets and the connections between them. To do this, we have a number of propositions whose proofs are often quite simple. The propositions are there to create a mental picture of the graphs.

The literature we refer to discusses non-wandering sets, whereas we investigate chain-recurrent sets. The biggest difference between these two approaches occurs at the final parameter value of each window. At those values, there is a chaotic attractor, consisting of intervals, and a repelling Cantor set, and these two non-wandering sets have a common periodic orbit. There is a single node, consisting in a finite union of intervals, that includes both non-wandering sets and the gaps in the Cantor set.

Notice, finally, that in all our proofs below we never use any property specific to the logistic map but rather those that come from it being a S-unimodal map. Hence, all our results actually hold in general for any S-unimodal map.

3.1. **Invariant sets of the logistic map.** The classification of attractors and repellors of S-unimodal and unimodal maps was an important achievement of 1-dimensional dynamics. Below we recall these results, that we state for the specific case of the logistic map, since they are the starting point of our work and we are going refer to them often in the remainder of this section.

Attractors. The first fundamental result found about attractors in S-unimodal maps is the uniqueness of periodic attractors.

Definition 3.1. The **immediate basin** of an attracting periodic orbit is the union of all connected components of the basin of the orbit that contain a point of it.

Singer Theorem 1 (Singer, 1978 [33])**.** If ℓ_μ has an attracting periodic orbit P, then it has no other attracting periodic orbit and the critical point c belongs to the immediate basin of P.

The classification of attractors and their uniqueness was proved by Guckenheimer in case of S-unimodal maps and by Jonker and Rand in case of unimodal maps (see also Thm. 4.1 in [11]).

Definition 3.2. By a **trapping region** we mean a collection $\mathcal{T}$ of k intervals with disjoint interiors $J_1, \ell_\mu(J_1), \ldots, \ell_\mu^{k-1}(J_1)$ such that:

1. $c \in \text{int}(J_1)$;
2. $\ell_\mu^k(J_1) \subset J_1$.

We denote by J_i the sets $\ell_\mu^{i-1}(J_1)$, $1 \le i \le k$, and by $J^{int} = J^{int}(\mathcal{T})$ the union of the interiors of the J_i.

It is unusual to ask that c belongs to the trapping region but this restriction is automatically satisfied for the trapping regions we are interested in.

Attractor Theorem 1 (Guckenheimer, 1979 [17]; Jonker and Rand, 1980 [23])**.** The map ℓ_μ has exactly one attractor and this attractor is one of the following types:

1. **Periodic**; this attractor is a periodic orbit. This case includes when the orbit attracts only from one side;
2. **Chaotic**; this attractor is a trapping region with a dense trajectory.
3. **Almost Periodic** [27], also sometimes called "odometer" or "solenoid"; this attractor is a Cantor set on which ℓ_μ acts as an adding machine (e.g. see Chap. 2 in [6]).

The basin of attraction has full measure in all three cases but only in the first two does the basin have non-empty interior. The critical point c is always in the basin.

Bifurcation plots showing the dependence of the attractor on the parameter μ for values to the left of the so-called **Myrberg-Feigenbaum** parameter value $\mu_{FM} \simeq 3.5699$ [13] appeared in several publications in the 1970's but, to the best of our knowledge, the first picture of the full bifurcation diagram appeared first in an article by Grebogi, Ott and Yorke in 1982 [15].

The almost periodic case occurs for those parameter values for which the graph has infinitely many nodes. For each point x_0 in the Cantor set attractor and each $\varepsilon > 0$, there is a periodic point x_ε such that the n-th iterate of the map on x_0 and the n-th iterate of the map on x_ε stay within ε of each other for all time $n \ge 0$. At μ_{FM}, every period orbit has period 2^k for some k and none of them belongs to the Cantor set. They converge to the Cantor set attractor as $k \to \infty$.

We write the parameter space as $(1, 4] = \mathcal{A}_P \cup \mathcal{A}_C \cup \mathcal{A}_{AP}$, where the union is disjoint, $\mathcal{A}_P$ is the set of parameters for which the attractor is a periodic orbit that is not a one-sided attractor, $\mathcal{A}_{AP}$ the set of those for which it is a Cantor set and $\mathcal{A}_C$ is the set of all other parameters, which includes all those for which the attractor is chaotic. The set $\mathcal{A}_P$ is open, a trivial consequence of the stability of periodic orbits under small perturbations, and dense, as proved independently by Lyubich [24] and Graczyk and Swiatek [14]. The complement of $\mathcal{A}_P$ is a Cantor subset of $[\mu_{FM}, 4]$. Notice that $\mu_{FM} \in \mathcal{A}_{AP}$ and $4 \in \mathcal{A}_C$. Jakobson [22] proved in 1981 that $\mathcal{A}_C$ has positive measure. It was proved in 2002 by Lyubich [25] that $\mathcal{A}_{AP}$ has measure zero.

Repellors. We come now to the results about the decomposition of the whole non-wandering set of ℓ_μ, which we denote by Ω_{ℓ_μ}. This result is a generalization of the following well-known result of Smale (see Sec. I.6 in [35] for details) called "Spectral Decomposition for Diffeomorphisms". In this theorem, Smale showed that, for a smooth manifold M and a Axiom-A diffeomorphism f on M, there is a unique way to write non-wandering set Ω_f as the finite union of elementary pairwise disjoint components Ω_j, on each of which the map has a dense orbit.

Definition 3.3. We say that a set P equal to the finite union of k isolated periodic orbits is a **cascade segment** if the periodic orbits in P belong to the same cascade,

whose first orbit has period n, and their period are equal to $n, 2n, \ldots, 2^{k-1}n$ for some k.

Non-Wandering Theorem 1 (van Strien, 1981 [37])**.** Each ℓ_μ has $p+1$ trapping regions $\mathcal{T}_j$, where p can be infinite, such that the following properties hold:

1. $\ell_\mu(\mathrm{cl}(J^{int}(\mathcal{T}_j))) \subset J^{int}(\mathcal{T}_j)$ for all $0 \leq j < p$.
2. The $\mathcal{T}_j$ are nested: $\mathrm{cl}(J^{int}(\mathcal{T}_j)) \subset \mathrm{cl}(J^{int}(\mathcal{T}_{j-1}))$ for all finite $1 \leq j \leq p$.
3. Set $K_j = \mathrm{cl}(J^{int}(\mathcal{T}_{j-1})) \setminus \mathrm{cl}(J^{int}(\mathcal{T}_j))$. Then Ω_{ℓ_μ} is the union of the following $p+1$ closed forward invariant sets:
$$\Omega_j = \bigcap_{n\geq 0} \ell_\mu^n\left(K_j\right), 0 \leq j < p,$$
$$\Omega_p = \Omega_{\ell_\mu} \cap \left[\bigcap_{j=0}^{p} \mathrm{cl}(J^{int}(\mathcal{T}_j))\right].$$
4. $\Omega_0 = \{0\}$;
5. Each Ω_j, $0 < j < p$, is the union of a Cantor set C_j and a cascade segment. The action of ℓ_μ on C_j is a subshift of finite type with a dense orbit.
6. Each Ω_j is hyperbolically repelling for $j < p$;
7. Ω_p is the unique attractor of ℓ_μ and it is not, in general, hyperbolic [Authors' note: the attractor fails to be hyperbolic at the beginning and end of each window, see Prop. 7)].
8. $\Omega_i \cap \Omega_j = \emptyset$ for $0 \leq i, j < p$ with $i \neq j$.
9. When $p < \infty$, $\Omega_{p-1} \cap \Omega_p$ is empty except when Ω_p is not hyperbolic, in which case it contains a single periodic orbit.
10. When $p = \infty$, all Ω_j are disjoint, Ω_∞ is a Cantor set and the action of ℓ_μ on it is an adding machine.

The first version of this theorem was given by Jonker and Rand [23] in case of unimodal maps. The specialization, used in the statement above, to S-unimodal maps is due to van Strien [37]. Several other versions and generalizations of this theorem are available in literature, *e.g.* Holmes and Whitley [20], Blokh and Lyubich [4], Blokh [3], Sharkovsky et al. [32]. Possibly the most thorough version is Thm. 4.2 in [12] by van Strien and de Melo.

To our knowledge, no bifurcation diagram showing a repelling Cantor set has appeared to date in literature. Our Fig. 1 and 2 illustrate the content of the theorem above by showing the attractors (in shades of grey) together with some repelling periodic orbits (in green) and Cantor sets (in red and blue).

The Non-Wandering Theorem above has some shortcoming for our purposes, e.g.: 1) the problem of what determines the number of cyclic trapping regions of ℓ_μ is not addressed; 2) unlike the nodes in our approach, the decomposition sets Ω_i are not necessarily pairwise disjoint; 3) nothing is explicitly stated about the dynamics of points outside the basin of attraction of the attractor; 4) the decomposition sets Ω_j contain, in general, more than one node. In particular, the restriction of the logistic map to them cannot a dense orbit, how happens instead in case of Axiom-A diffeomorphisms. In the remainder of this section we show that these shortcomings naturally disappear by replacing Ω_{ℓ_μ} with $\mathcal{R}_{\ell_\mu}$.

Homtervals. We recall a last theorem that we are going to use several times in this section.

Definition 3.4. A closed interval $J \subset [0,1]$ is a **homterval** for ℓ_μ if c is not in the interior of $\ell_\mu^k(J)$ for any integer $k \geq 0$.

Notice that, equivalently, J is a homterval for ℓ_μ if all of its iterates ℓ_μ^k, $k = 0, 1, \ldots$, are strictly monotonic on J.

Homterval Theorem 1 (Guckenheimer, 1979 [17])**.** Assume that ℓ_μ admits a homterval J. Then the attractor of ℓ_μ is periodic and $\omega(x)$ is a periodic orbit for each $x \in J$.

Notice that, in particular, $\omega(x)$ must be equal to the attractor for almost all points of J.

The following case is particularly important to us. When a period-k orbit is attracting for some μ_0, and then μ is increased so that the periodic orbit becomes unstable, it period-doubles at some μ_1. Then, at some $\mu_2 > \mu_1$, the new attracting period-$2k$ orbit is superstable. For each $\mu \in (\mu_1, \mu_2]$, each point z of the now-repelling period-k orbit lies in an interval K_z whose endpoints are period-$2k$ points. K_z is a homterval that is invariant under ℓ_μ^k. In particular, all points in the homterval K_z, except z, are attracted to the period-$2k$ orbit.

3.2. **Chain-recurrence and graph for the logistic map.** This subsection contains our contributions for this article. We start by introducing cyclic trapping regions (Def. 3.5), a kind of trapping region having a periodic orbit on its boundary. Cyclic trapping regions and their "accessible" periodic orbits (Def. 3.14) come in two flavors: regular and flip (Def. 3.6).

Pairing windows and regular trapping regions. For the logistic map, there is a 1-1 correspondence that pairs each repelling regular trapping region with a "window" in the bifurcation diagram (see Fig. 1 for the full diagram and Fig. 2 for a detail of the period-3 window). A window is a maximal interval $[\mu_0, \mu_1]$ that has a regular cyclic trapping region that persists throughout the interval. The observed cascade of the window lies within the cyclic trapping region. Every window comes with a node which is the invariant Cantor set of chain-recurrent points that do not fall into the trapping region. Figure 2 shows, for each value of μ, the Cantor set of the period-3 window (in red) and the one of its period-9 subwindow (in blue). For each μ, the largest white gap in the Cantor set is one of the intervals of the regular trapping region corresponding to that window, which we call J_1. The number of such intervals, namely the period of the cyclic trapping region, coincides with the period of the window and with the period of the orbit at the boundary of the trapping region. This orbit is the unique "accessible" orbit of the Cantor set (see Def. 3.14 and Thm. 3.15).

A period-$2k$ flip trapping region is created as μ increases when the derivative at the period-k point $\frac{d}{dx}\ell_\mu^k(p_1)$ becomes negative (see Fig. 3).

We show that each repelling node is either a Cantor set, in case the corresponding cyclic trapping region is regular, or a flip periodic orbit, in case is flip (Prop. 6). We give an analogue classification of attracting nodes (Prop. 7).

We use cyclic trapping regions to study the structure and properties of the nodes and edges of the graph of ℓ_μ. Here are some key structural results:

- **Each node has its own trapping region.** Given a node N, the minimum distance between N and c is achieved at a period-k point p_1 in N and the map ℓ_μ^{2k} leaves invariant the interval J_1 with endpoints p_1 and $1 - p_1$ (Prop. 4). The interval J_1 it is one of the intervals of a cyclic trapping region $\mathcal{T}(N)$. The

period of the trapping region is k if it is regular and $2k$ if it is flip. It follows that no point of N falls under the map into the interior of the trapping region.

- **Each trapping region has its own node.** Given a cyclic trapping region $\mathcal{T}$, its interval J_1 contains the critical point. There is a unique node $\mathrm{Node}(\mathcal{T})$ containing the periodic orbit (passing through p_1) at its boundary (Def. 3.11).
- **The trapping region and the node have one periodic orbit in common.** The point p_1 belongs to this periodic orbit.
- **Given any two distinct nodes N and N', one must be in the trapping region of the other.** Specifically, if $p_1(N)$ is closer to c than $p_1(N')$, then N is in the trapping region of N'.
- **The graph is a tower.** For each chain-recurrent point $x \in J^{int}(N)$, there is a trajectory t passing through x that converges backwards to $p_1(N)$ (Prop. 8). This means that there is an edge between each pair of nodes, namely the graph is a tower (Thm 3.16). This tower is infinite if and only if $\mu \in \mathcal{A}_{AP}$. In Figs. 1 and 2 we show several examples of towers in the logistic map.

Windows. We start by introducing and refining some fundamental concepts that will be in the background of all statements in this section.

Definition 3.5. A **period-k (cyclic) trapping region** is a trapping region $\mathcal{T} = \{J_1, \ell_\mu(J_1), \dots, \ell_\mu^{k-1}(J_1)\}$ such that J_1 has endpoints p_1 and $q_1 = 1 - p_1$ and the one denoted by p_1 is periodic. We denote by $|\mathcal{T}|$ the period of $\mathcal{T}$ and by $\mathrm{orbit}(\mathcal{T})$ the periodic orbit containing p_1.

Remark 1. The requirement that each interval of a period-k trapping region be an iterate of J_1 can be relaxed by allowing each J_i to be larger than $\ell_\mu(J_{i-1})$, as long as $\ell_\mu(J_k) \subset J_1$. For such generalized trapping region, therefore, we have that $\ell_\mu(J_i) \subset J_{i+1}$ for all i, where we identify J_{k+1} with J_1.

There are two limiting cases. One is the standard trapping region defined above, when all inclusions are equalities except for the last one: $\ell_\mu(J_k) \subset J_1$. This choice is minimal: if any J_i, $i \neq 1$, is taken smaller, then there is no trapping region with that J_1 and that J_i. The other one is the one where all inclusions are equalities except for the first one: $\ell_\mu(J_1) \subset J_2$. This choice is maximal: if J_2 were chosen any larger, $\ell_\mu(J_k)$ would be larger than J_1. In a maximal trapping region ℓ_μ, restricted to any J_i, sends interiors into interiors and endpoints into endpoints.

The results of this section do not depend on which particular definition of trapping region is used. In Prop. 6 and in the pictures we use the "maximal" definition because it is more convenient.

As Figs. 8 and 9 suggest, there are two distinct kinds of cyclic trapping regions.

Definition 3.6. Let $\mathcal{T}$ be a cyclic trapping region of ℓ_μ such that $\mathrm{orbit}(\mathcal{T})$ is a period-k orbit. Denote by D be the value of the derivative of ℓ_μ^k at any points of $\mathrm{orbit}(\mathcal{T})$; the value does not depend on the point chosen.

If $D > 0$, we call $\mathrm{orbit}(\mathcal{T})$ a **regular orbit** and $\mathcal{T}$ is a **regular (cyclic) trapping region**. In this case $|\mathcal{T}| = k$.

If $D < 0$, we call $\mathrm{orbit}(\mathcal{T})$ a **flip orbit** and $\mathcal{T}$ is a **flip (cyclic) trapping region**. In this case $|\mathcal{T}| = 2k$.

The case $D = 0$ is degenerate.

Notice that, since periodic orbits are stable with respect to small perturbations, a trapping region $\mathcal{T} = \mathcal{T}_\mu$ depends continuously on μ.

Definition 3.7. For any trapping region $\mathcal{T}$, we denote by $\mathbf{Range}(\mathcal{T}) = [\boldsymbol{\mu_0}, \boldsymbol{\mu_1}]$ the closed maximal μ interval on which $\mathcal{T} = \mathcal{T}_\mu$ can be defined continuously and write $p_1 = p_1(\mu)$ for the periodic point on the boundary of $J_1 = J_1(\mathcal{T}_\mu)$. We say that $\mathcal{T}_\mu$ is a 1-parametric family of regular trapping regions when it is a regular cyclic trapping region for every $\mu \in \text{Range}(\mathcal{T})$. We say that $\mathcal{T}_\mu$ is a 1-parametric family of flip trapping regions when it is a regular cyclic trapping region for at least a value $\mu \in (\mu_0, \mu_1)$.

Beginning and end of (a family of) trapping regions.

Let $\mathcal{T}$ be a regular trapping region. When orbit($\mathcal{T}$) is repelling, the family begins at $\mu = \mu_0$ with an attractor-repellor bifurcation point with $D = +1$. An example is shown in Fig. 7 in case of the period-3 window, where μ_0 and μ_1 are labeled μ_{7b} and μ_{7e}, where b and e are for beginning and end. Each node has its own p_1, q_1 and J_1 and to distinguish between them we use primes and double primes. A pair of period-3 orbits $\mathcal{O}'$, given by $p'_1 \mapsto p'_2 \mapsto p'_3 \mapsto p'_1$, and $\mathcal{O}$, given by $p_1 \mapsto p_2 \mapsto p_3 \mapsto p_1$, arises at $\mu_{7b} = 1 + 2\sqrt{2} \simeq 3.828$. $\mathcal{O}'$ is attracting until period-doubling, $\mathcal{O}$ is always repelling. The two orbits coincide at μ_{7b}. Notice that there is no other such pair of period-3 orbits for the logistic map.

There is a period-3 regular trapping region $\mathcal{T}$ for which $\mathcal{O}$ lies on its boundary. We show in red, at $\mu = \mu_{71}$, the interval J_1 of $\mathcal{T}$. At $\mu_{73} \simeq 3.846$, we show the interval J_1 above and, written over it in blue, the intervals J'_4 (top), J'_1 (center) and J'_7 (bottom) of a period-9 regular trapping region $\mathcal{T}'$ that is nested in $\mathcal{T}$. The ends of these blue intervals, not labeled in the picture, have black dots. Notice that the J_1 intervals of all cyclic trapping regions are all symmetric with respect to c and so are all one inside the other; correspondingly, given any two cyclic trapping regions $\mathcal{T}$ and $\mathcal{T}'$, the intervals of one are all strictly contained in the intervals of the other.

The family ends at $\mu = \mu_1$, when c falls eventually on orbit($\mathcal{T}_\mu$), namely on $\mathcal{O}$ (but c does not belong to $\mathcal{O}$). An example is the case $\mu = \mu_{7e} \simeq 3.8568$ in Fig. 7.

When orbit($\mathcal{T}$) is attracting, at $\mu = \mu_0$, an orbit, orbit($\mathcal{T}_{\mu_0}$), of period k is created, for some k, with $D = +1$. Such case is shown in Fig. 3 at $\mu = 1$, where the fixed point p_1 of ℓ_μ arises. Caution: if the orbit is created at a period-doubling bifurcation, k means the period of the newly created, period-doubled, orbit. The trapping region $\mathcal{T}$ ends, at $\mu = \mu_1$, at the super-stable point, namely c belongs to orbit($\mathcal{T}_{\mu_1}$). Examples are shown in Fig. 3, at $\mu = 2$, and in Fig. 7, at $\mu = \mu_{7ss} \simeq 3.832$. Strictly speaking, at $\mu = \mu_1$ the trapping region is degenerate since each interval collapses into a point.

Let $\mathcal{T}$ be a flip trapping region. Such a family always starts at a super-stable point, where the trapping region is degenerate. Examples are shown in Fig. 3, where the attracting fixed point p_1 is superstable at $\mu = 2$, and in Fig. 7, where p'_1 belongs to $\mathcal{O}'$, whose super-stable point is $\mu_{7ss} \simeq 3.832$. Close enough to the super-stable point, orbit($\mathcal{T}_\mu$) is attracting (see the period-2 flip trapping region in Fig. 3).

At some $\bar{\mu} \in (\mu_0, \mu_1)$, orbit($\mathcal{T}_\mu$) has a period-doubling bifurcation point and becomes repelling. In Fig. 6 we show several examples of flip trapping regions with a repelling periodic orbit at their boundary. At $\mu = \mu_{60}$, there is only one such trapping region $\mathcal{T} = \{J_1, J_2\}$. Here $J_1 = [q_1, p_1]$ and $J_2 = [p_1, q_2]$, where p_1 is the flip fixed point of the logistic map, $q_1 = 1 - p_1$ and $\ell_\mu(q_2) = q_1$. Both J_1 and J_2 are painted in red. At $\mu = \mu_{61}$, a second flip trapping region $\mathcal{T}' = \{J'_1, \ldots, J'_4\}$ arises, where $J'_1 = [p'_1, q'_1]$, $J'_2 = [p'_2, q'_2]$, $J_3 = [q'_3, p_1]$ and $J'_4 = [q'_4, p'_2]$. In this case, p'_1, p'_2 is a period-2 orbit, $\ell^2_\mu(q'_3) = q'_1$ and $\ell^2_\mu(q'_4) = q'_2$. This trapping region is painted in blue and its intervals J'_i are proper subsets of the J_i.

At $\mu = \mu_{62}$, a third flip trapping region $\mathcal{T}' = \{J'_1, \dots, J'_8\}$ arises, where $J''_1 = [q''_1, p''_1]$ and so on. The J''_i are painted in dark green. At their boundaries lie the period-4 orbit $p''_1, \dots, p''_4$. In this case, $\ell^4_\mu(q'_5) = q'_1$ and so on. Another example is provided in Fig. 7 at $\mu = \mu_{72}$. The intervals J'_1, J'_4 shown, which are part of a period-6 flip trapping region of ℓ_μ, are a period-2 flip trapping region for ℓ^3_μ.

The family ends, at $\mu = \mu_{\text{Merge}}$, when c falls eventually on orbit$(\mathcal{T}_\mu)$ (but it is not super-stable). In this special case, all endpoints of the J_i are on the orbit of c. In Fig. 3 we mark with a cyan vertical line the point

$$\mu_M = 3[1 + (19 - 3\sqrt{33})^{1/3} + (19 + 3\sqrt{33})^{1/3}]/2 \simeq 3.67857. \tag{3}$$

This value marks the end of the flip trapping region $\mathcal{T}$ with orbit$(\mathcal{T}) = \mathcal{O}$. At μ_M, we have that $\ell_\mu(c) = q_2$, $\ell^2_\mu(c) = q_1$, and $\ell^3_\mu(c) = p_1$. In Fig. 7 we do the same with the point $\mu_{7M} \simeq 3.851$. This value marks the end of the flip trapping region $\mathcal{T}'$ such that orbit$(\mathcal{T}') = \mathcal{O}'$.

We now define the well-known concept of a window in a bifurcation diagram. We define it from an unusual point of view which emphasizes the importance of trapping regions. A window is where a particular kind of trapping region exists.

Definition 3.8. Let $\mathcal{T}$ be a period-k regular trapping region such that orbit$(\mathcal{T})$ is repelling. Let the μ-interval W be the (maximal) range of $\mathcal{T}$. We say that W is a **period-k window**. When a period-k_1 window W_1 contains a period-k_2 window W_2, with $k_2 \geq k_1$, we say that W_2 is a **subwindow** of W_1. Notice that k_2 is a multiple of k_1.

We will show in Prop. 5 that, if $W_1 = \text{Range}(\mathcal{T}_1)$ and $W_2 = \text{Range}(\mathcal{T}_2)$ and both orbit$(\mathcal{T}_1)$ and orbit$(\mathcal{T}_2)$ are repelling, then $k_2 > k_1$.

Nodes. Here we will study in detail nodes and their relation with cyclic trapping regions. We will show that each node is paired with a cyclic trapping region and this cyclic trapping region has always a periodic orbit of the node on its boundary. This will enable us to classify all repelling and attracting nodes of the logistic map.

Definition 3.9. Given a node N of ℓ_μ, we denote by $\rho(N)$ its minimum distance from the critical point c. We write $N_1 > N_2$ if $\rho(N_1) > \rho(N_2)$.

Notice that $\rho(N) > 0$ for every repelling node. In contrast, $\rho(N) = 0$ only if N contains a chaotic attractor or an almost periodic attractor or a superstable periodic attractor.

We will show in the remainder of the section that $N_1 > N_2$ implies that N_1 is upstream from N_2. For the logistic map, this is ultimately equivalent to the fact that the graph is a tower. We start by showing that ρ is injective.

Proposition 2. *Let N_1 and N_2 be two distinct nodes. Then either $N_1 > N_2$ or $N_2 > N_1$.*

Proof. Let p_0 be a point of N such that $|p_0 - c| = \rho(N)$. The other point having distance $\rho(N)$ from c is $1 - p_0$. Since $\ell_\mu(1 - p_0) = \ell_\mu(p_0) \in N$, then $1 - p_0$ is either in the node or in its preimage and therefore it cannot belong to any other node. Hence, no two nodes are equidistant from c. □

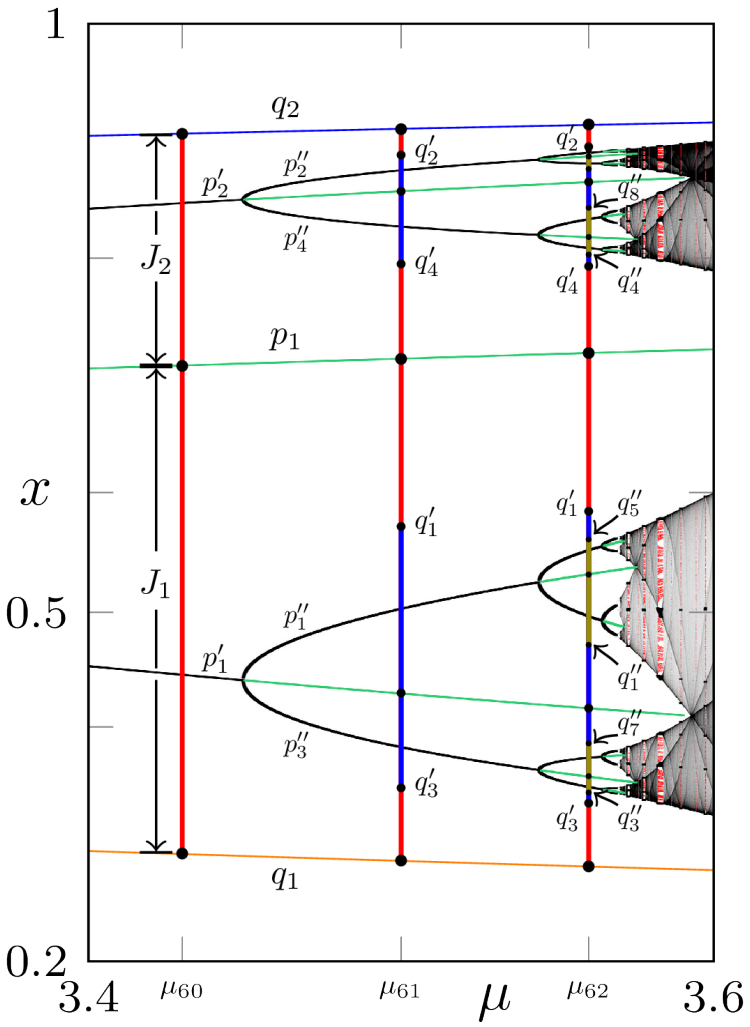

FIGURE 6. **Flip trapping regions of the logistic map.** This picture is a blowup of Fig. 3. It shows at the three parameter values $\mu_{60} = 3.43, \mu_{61} = 3.5, \mu_{62} = 3.56$, all flip cyclic trapping regions of the logistic map with a repelling orbit at their boundary. At $\mu = \mu_{60}$, there is a single flip trapping region $\mathcal{T} = \{J_1, J_2\}$, where $J_1 = [q_1, p_1]$ and $J_2 = [p_1, q_2]$. The point p_1 is the flip fixed point, $q_1 = 1 - p_1$ and $\ell_\mu(q_2) = q_1$. A description for the other two values of μ is given in the text below Def. 3.7.

Definition 3.10. Let N be a node of ℓ_μ with $\rho(N) > 0$. From now on, $\boldsymbol{p_0 = p_0(N)}$ will refer to a point in N with minimal distance from c. We denote by $\boldsymbol{J_1(N)}$ the closed interval with endpoints p_0 and $1 - p_0$.

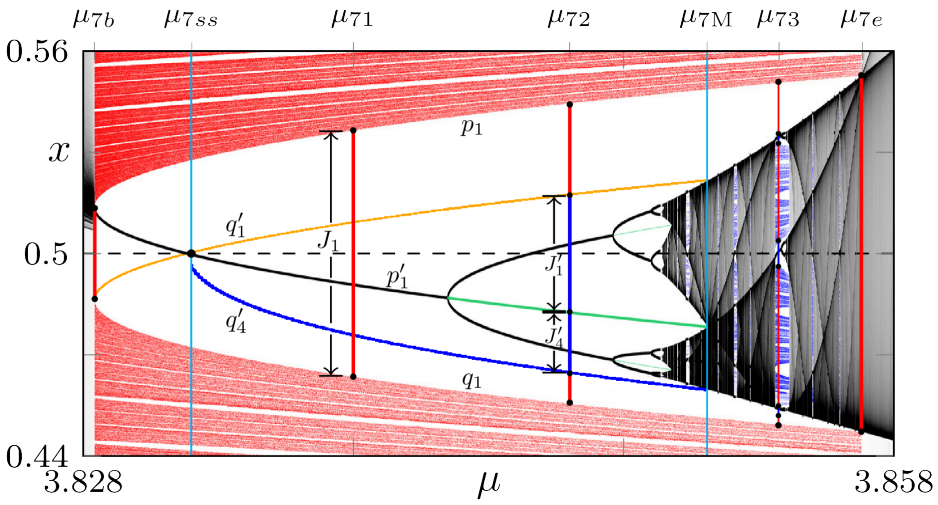

FIGURE 7. **Examples of regular and flip cyclic trapping regions.** In this detail of the period-3 window, the curve of points denoted by p_1 is a period-3 repellor. It separates the red Cantor set from the white basin of the attractor. The curve of points $q_1 = 1 - p_1$ separates the Cantor set from the basin. A description for the marked values of μ is given in the text below Def. 3.7.

We will later show that one and only one of the two is periodic and we will later refer to the periodic one as p_1. In Figs. 6 and 7 we show sets J_1, together with the corresponding endpoint p_1, for several nodes.

Proposition 3 (Downstream Proposition)**.** *Let N be a node of ℓ_μ with $\rho(N) > 0$. Then each chain-recurrent point in $J_1(N)$ is downstream from N.*

Proof. Assume, for discussion sake, that $p_0 < c$; the argument for $p_0 > c$ is virtually the same. We set $K = K_\varepsilon = [p_0, p_0 + \varepsilon]$.

There are two cases.

CASE 1: Assume that for every $\varepsilon > 0$, for some $r > 1$, $\ell_\mu^r(K_\varepsilon)$ contains c in its interior.

Since p_0 is the closest point of N to c, $\ell_\mu^r(p_0)$ cannot be in the interior of $J_1(N)$. Then $\ell_\mu^r(K_\varepsilon)$ must contain at least either $[p_0, c]$ or $[c, 1-p_0]$. Denote by J_0 the half of J_1 that K_ε eventually maps onto for arbitrarily small ε. Hence, for arbitrarily small ε, there are ε-chains from p_0 to each point within J_0. Notice that chain-recurrent points x and $1 - x$ belong to the same node and that, if p_0 is upstream from any point of a node, is upstream from each point of that node.

CASE 2: Assume that, for some $\varepsilon > 0$ and all $r > 1$, $\ell_\mu^r(K_\varepsilon)$ does not contain c in its interior. In particular, the attractor must be a periodic orbit by the Homterval Theorem.

If N contains non-periodic points, let p be one of them and assume, by discussion sake, that $p < c$. Then $[p, p+\varepsilon]$ cannot be a homterval and so, for the same argument above, every point of $J_1(N)$ is downstream from N.

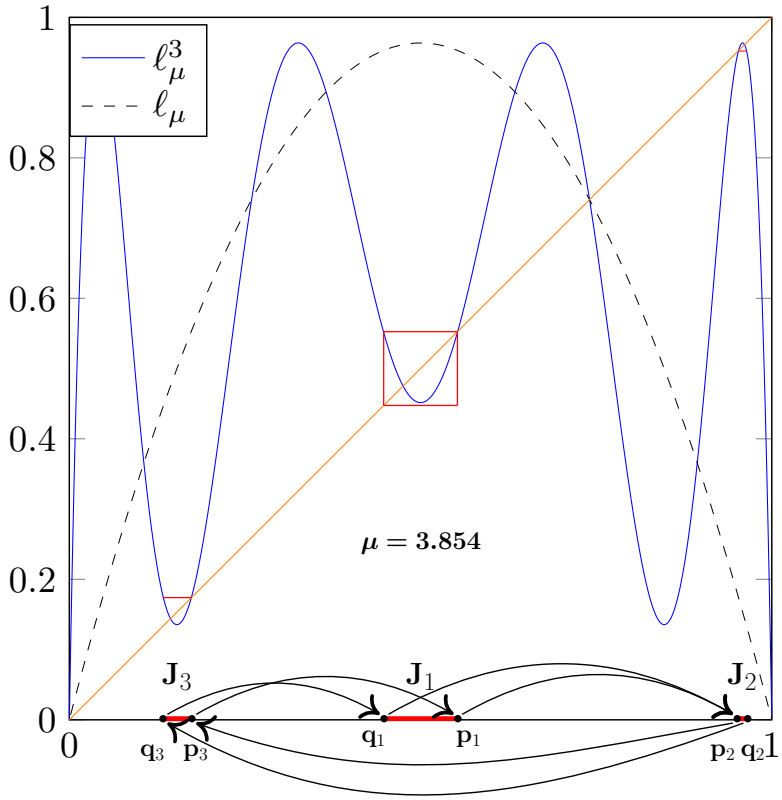

FIGURE 8. **A regular cyclic trapping region** for the logistic map. The bifurcation diagram for the logistic map has a period-3 window in parameter space starting at $\mu_0 = 1 + \sqrt{8} \simeq 3.828$, where a pair of an attracting and a repelling period-3 orbits arise, and ending at $\mu_1 \simeq 3.857$, where the unstable periodic orbit collides with the attractor (i.e. there is a *crises* [15]). Here we show what is happening at one of the intermediate parameter values, $\mu = 3.854$. There are intervals J_i with endpoints q_i, p_i, $i = 1, 2, 3$, shown in red, which, together, form a period-3 regular cyclic trapping region for ℓ_μ (Def. 3.5). The arrows show how the endpoints map under ℓ_μ. The intervals are chosen so that $p_1 \mapsto p_2 \mapsto p_3 \mapsto p_1$ is an unstable period-3 orbit and $\ell_\mu^3(q_i) = p_i$ for $i = 1, 2, 3$. This construction gives rise to a cyclic trapping region because, for this value of μ and this choice of the endpoints, $\ell_\mu^3(J_i) \subset J_i$. The picture also includes the graph of $\ell_\mu^3(x)$ and $\ell_\mu(x)$.

If all points of N are periodic, then p_0 belongs to a period-k orbit and K_ε lies in a maximal homterval we denote by H. So H is invariant under ℓ_μ^{2k}, which is orientation preserving. If $h \in H$ and it is not a fixed point for ℓ_μ^{2k}, then h converges to an attractor, and there is only one attractor for ℓ_μ. So the attractor is a periodic-$2k$ orbit. By Singer theorem, there is an interval H_c in the basin of this orbit that

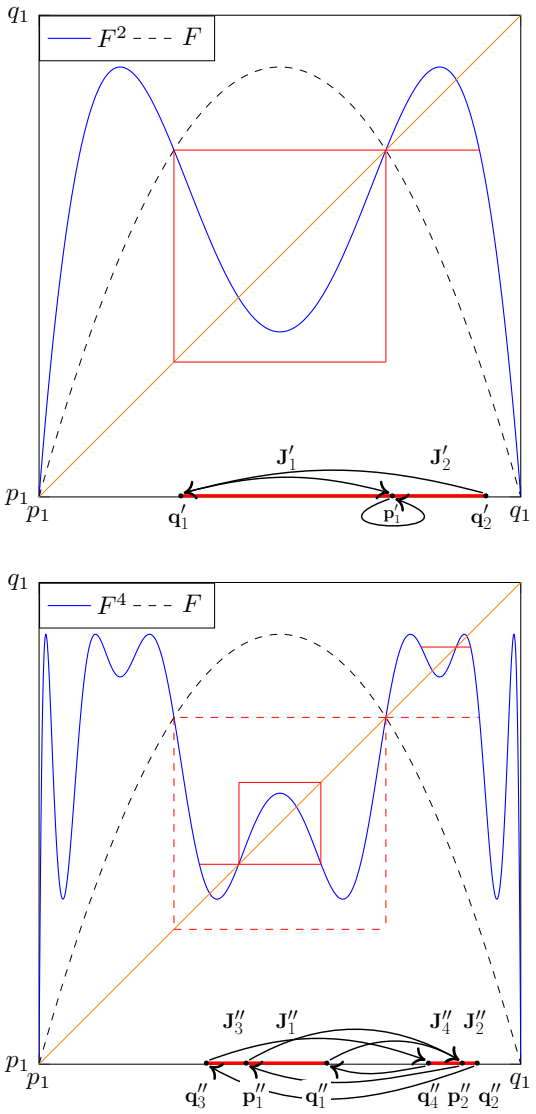

FIGURE 9. **Nested flip cyclic trapping regions** for the logistic map. On the left panel, we show an interval $[p_1, q_1]$ that is the J_1 interval of a period-k cyclic trapping region $\mathcal{T}$ for $F = \ell_\mu^k$. Inside J_1, we show a flip cyclic trapping region (Def. 3.5) $\mathcal{T}' = \{J'_1, J'_2\}$, where $J'_1 = [q'_1, p'_1]$ and $J'_2 = [p'_1, q'_2]$. On the right panel, again inside J_1, we show a flip cyclic trapping region $\mathcal{T}'' = \{J''_1, J''_2, J''_3, J''_4\}$ nested in $\mathcal{T}'$, where $J''_1 = [p''_1, q''_1]$, $J''_2 = [p''_2, q''_2]$, $J''_3 = [q''_3, p''_1]$ and $J''_4 = [q''_4, p''_2]$. The arrows in both panels show how the endpoints map under F. On the left, the periodic orbit at the boundary of the cyclic trapping region is the fixed point p'_1, on the right is the period-2 orbit $p''_1 \mapsto p''_2 \mapsto p''_1$. Notice that $F^2(J'_1) \subset J'_1$ and $F^4(J''_1) \subset J''_1$. The picture also includes the graphs of $F(x)$, $F^2(x)$ and $F^4(x)$. The actual value used in these pictures is $\mu = \mu_{FM}$; at this value, there is an infinite sequence of flip cyclic trapping regions nested one into the other.

contains both c and a point q_0 of the period-$2k$ orbit. We can assume H_c is the largest open interval that is in the basin and contains c. From the construction, the boundary of H_c contains a period-k point p^*. The other boundary point is $1-p^*$. So p^* is the closest point of N to c. Hence, either $p^* = p_0$ or $p^* = 1 - p_0$ and so $J_1(N) = H_c$.

In particular, the open interval with endpoints q_0 and $1 - q_0$ is a subset of the basin of attraction of the attractor and therefore does not contain any chain-recurrent point. Hence, by the same argument above, all chain-recurrent points in $J_1(N)$ are downstream from N. □

The proof above implies, in particular, the following:

Corollary 1. *Let N be a node of ℓ_μ with $\rho(N) > 0$. Then there is no point in the interior of $J_1(N)$ that falls eventually into N.*

Proof. A point falling eventually on N is upstream from N. By Prop. 3, all chain-recurrent points of $J_1(N)$ are downstream from N, so a point in the interior of $J_1(N)$ falling eventually into N would be both upstream and downstream from N and so it would belong to N. This is not possible because, by hypothesis, p_0 is the closest point of N to c. □

Definition 3.11. We denote by $\mathrm{Node}(\mathcal{T})$ the node that contains $\mathrm{orbit}(\mathcal{T})$.

The node $\mathrm{Node}(\mathcal{T})$ contains no points of $J^{int}(\mathcal{T})$, in fact it is the node closest to c with this property. Notice that $\rho(\mathrm{Node}(\mathcal{T})) > 0$ unless $\mathrm{orbit}(\mathcal{T})$ is attracting and c lies on it. We are now in position to show that this map from cyclic trapping regions to nodes with strictly positive distance from c can be inverted.

Proposition 4 (The cyclic trapping region of a node)**.** *Let N be a node of ℓ_μ with $\rho(N) > 0$. Let $p_0 = p_0(N)$. Then:*

1. *Either p_0 or $1 - p_0$ is a periodic point. Let k denote its period.*
2. *There is a cyclic trapping region $\{J_1, \dots, J_r\}$, where $J_1 = J_1(N)$, whose period r is either k or $2k$.*

Notice that $\ell_\mu^r(p_0) = \ell_\mu^r(1 - p_0)$ for all $r \geq 1$.

Proof. Let $J_0 = J_1(N) \cap [0, c]$ and denote by J_1^{o} the interior of $J_1(N)$.

Assume first that the attractor is chaotic or almost periodic. Then there cannot be homtervals and, by the Homterval Theorem, there is some $k \geq 1$ such that $\ell_\mu^k(J_0) = \ell_\mu^k(J_1)$ contains c in its interior. In other words, there is a point x in J_1^{o} such that $\ell_\mu^k(x) = c \in J_1^{\mathrm{o}}$.

We claim that this is enough to grant that J_1^{o} is invariant under ℓ_μ^k. Indeed, by continuity, if there were a $y \in J_1^{\mathrm{o}}$ with $\ell_\mu^k(y) \notin J_1^{\mathrm{o}}$, there would be some $\xi \in J_1^{\mathrm{o}}$ between x and y such that either $\ell_\mu^k(\xi) = p_0$ or $\ell_\mu^k(\xi) = 1 - p_0$. This, though, is impossible because, by our Downstream Proposition, there are no preiterates of N in J_1^{o}. Moreover, by continuity, the common value of p_0 and $1 - p_0$ under ℓ_μ^k must belong to $J_1(N)$ and, since N is forward invariant and there are no points of N in J_1^{o}, it can only be either p_0 or $1 - p_0$, so the theorem is proved in this case.

Assume now that the attractor is a period-r orbit. Then (see the corollary above) there is a point q_0 of the attractor in J_1. Hence $\ell_\mu^r(q_0) = q_0$ and so, as above, there is a point in J_1^{o} whose image under ℓ_μ^r belongs to J_1^{o}. By the argument above, ℓ_μ^r leaves both J_1^{o} and $J^1(N)$ invariant, proving the theorem in this second case.

We have left it to the reader to show that the intervals $J_1, \ell_\mu(J_1), \dots, \ell_\mu^{r-1}(J_1)$ have disjoint interiors. □

Definition 3.12. We denote by $\boldsymbol{\mathcal{T}(N)}$ the trapping region with $J_1 = J_1(N)$.

Notice that $\mathcal{T}(N)$ is the largest cyclic trapping region that does not contain N in its interior.

A byproduct of Thm. 4 is that either p_0 or $1 - p_0$ is a periodic point:

Corollary 2. *The minimum distance between a repelling node N and c is achieved at the periodic point $p_1(\mathcal{T}(N))$.*

We sometimes denote that periodic point by $\boldsymbol{p_1(N)}$. In Fig. 6 we show all cyclic trapping regions corresponding to three parameters values at the left of the Feigenbaum-Myrberg point. The nodes corresponding to each trapping region are flip periodic orbits and therefore the trapping regions are flip cyclic trapping regions.

At μ_{60}, there are two repelling nodes N_0 and N_1, namely the fixed point 0 and the fixed point p_1, and an attracting node N_2 consisting of a period-2 orbit $p_1' = p_1(N_2), p_2'$. Since p_1 is a flip orbit, $\mathcal{T}(N_1) = \{J_1, J_2\}$ has period 2. The picture shows, in red, the intervals $J_1 = J_1(N_1)$, with endpoints $p_1 = p_1(N_1)$ and $q_1 = 1 - p_1$, and J_2, with endpoints p_1 and q_2, which is the larger root of $\ell_{\mu_{60}}(x) = q_1$.

As μ increases from μ_{60} to μ_{61}, the orbit p_1', p_2' bifurcates and becomes repelling, so that at μ_{61} there is now an attracting node N_3 consisting of a period-4 orbit $p_1'' = p_1(N_3), \dots, p_4''$. The picture shows, again in red, the intervals of $\mathcal{T}(N_1)$. Moreover it shows, in blue, the intervals $J_1' = J_1(N_2), \dots, J_4'$ of $\mathcal{T}(N_2)$. Similarly, as μ increases from μ_{61} to μ_{62}, the period-4 orbit bifurcates and becomes repelling, so that at μ_{62} there is now a period-8 attracting orbit. Here the picture shows, again in red and blue respectively, the intervals of $\mathcal{T}(N_1)$ and $\mathcal{T}(N_2)$. Moreover it shows, in olive green, the intervals $J_1'' = J_1(N_3), \dots, J_8''$ of $\mathcal{T}(N_3)$.

In Fig. 7, we show some example of regular cyclic trapping regions for some parameter values in the period-3 window. Notice that the picture shows only a detail close to the central cascade of the window.

At μ_{71}, there are two repelling nodes, $N_0 = \{0\}$ and N_1, the red Cantor set (see Figs. 1, 2), and an attracting one consisting in a period-3 orbit. The picture shows, in red, the interval $J_1 = J_1(N_1)$ of the regular period-3 cyclic trapping region $\mathcal{T}(N_1)$, whose endpoints are $p_1 = p_1(N_1)$ and $q_1 = 1 - p_1$. While increasing from μ_{71} to μ_{72}, the period-3 orbit bifurcates so that at μ_{72} we have now an attracting node N_3 consisting of a period-6 orbit. The picture shows the interval $J_1(N_1) = [q_1, p_1]$ and the intervals $J_1' = J_1(N_2) = [p_1', q_1']$, where $p_1' = p_1(N_2)$ and $q_1' = 1 - p_1'$, and $J_4' = [q_4', p_1']$ of the period-6 cyclic trapping region $\mathcal{T}(N_2)$.

Finally, at μ_{72}, there are three repelling nodes N_0, N_1, N_2, namely the fixed point 0, the red Cantor set and the blue Cantor set, and an attracting node N_4 consisting of a period-9 orbit. The picture shows the interval $J_1(N_1) = [p_1, q_1]$ of the regular period-3 cyclic trapping region $\mathcal{T}(N_1)$ and, in blue, the intervals $J_1' = J_1(N_2)$, not labeled in figure, J_4', J_7' of the regular period-9 cyclic trapping region $\mathcal{T}(N_2)$.

Since Prop. 4 shows that $\text{orbit}(\mathcal{T}_N) \subset N$, we have the following.

Corollary 3. *Let N be a node with $\rho(N) > 0$. Then $\text{Node}(\mathcal{T}_N) = N$.*

Notice that, in particular, since every cyclic trapping region $\mathcal{T}$ is characterized by the periodic orbit at its boundary, the number of cyclic trapping regions of a given ℓ_μ is bounded from above by the number of periodic orbits of the map. While

this bound is trivial for $\mu \geq \mu_{FM}$, where there are always infinitely many periodic orbits, it is actually sharp for $\mu < \mu_{FM}$. In this case, indeed, for each μ there is a $k \geq 0$ such that the set of all periodic orbits for ℓ_μ consists in a single orbit of period 2^i for $i = 0, \dots, k$.

Definition 3.13. We say that two repelling nodes $N_1 > N_2$ are **consecutive** if there is no node N_3 such that $N_1 > N_3 > N_2$.

Proposition 5. *Let $N_1 > N_2$ be two repelling nodes of ℓ_μ. Then:*

1. *$|\mathcal{T}(N_2)| > |\mathcal{T}(N_1)|$ and $|\mathcal{T}(N_1)|$ divides $|\mathcal{T}(N_2)|$;*
2. *$N_2 \subset J^{int}(N_1) \setminus J^{int}(N_2)$;*
3. *if N_1 and N_2 are consecutive, N_2 is the set of all chain-recurrent points in $J^{int}(N_1) \setminus J^{int}(N_2)$.*

Proof. **1.** Set $\mathcal{T}(N_1) = \{J_1, \dots, J_k\}$ and $\mathcal{T}(N_2) = \{J'_1, \dots, J'_{k'}\}$. Since the maps $\ell_\mu : J_i \to J_{i+1}$, $i = 2, \dots, k$ are all homeomorphisms, where we set $J_{k+1} = J_1$, then inside each J_i there must be the same number of intervals J'_i, namely $k' = mk$ for some integer $m \geq 1$.

Suppose now that $k' = k$ and assume, for discussion sake, that $p_1(N_1) < c$. Then, since $\ell_\mu^k(J'_1) \subset J'_1$, both $p_1(N_1)$ and $p_1(N_2)$ are fixed points for ℓ_μ^k.

If $p_1(N_2) < c$ as well, then N_2 would be an attracting node. Indeed, if it were not, there would be an attractor point x, belonging to an attracting node N_3, between $p_1(N_1)$ and $p_1(N_2)$. Hence N_2 would be inside $J^{int}(N_3)$ but, since N_3 is an attractor, $J^{int}(N_3)$ is a subset of the basin of N_3.

If, on the contrary, $p_1(N_2) > c$, then the derivative of ℓ_μ^k at $p_1(N_2)$ would be negative and therefore J'_1 cannot be invariant under ℓ_μ^k.

2. Since $N_1 > N_2$, there is at least one point of N_2 inside $J^{int}(N_1)$ and therefore, since both $J^{int}(N_1)$ and N_2 are forward-invariant, the whole N_2 must be contained in $J^{int}(N_1)$. Moreover, by construction, no point of N_2 can fall onto $J^{int}(N_2)$.

3. Suppose that there is a chain-recurrent point $x \in J^{int}(N_1) \setminus J^{int}(N_2)$ not belonging to N_2. Denote by N_3 the node x belongs to. Without loss of generality we can assume that $x \in J_1(N_1)$. Then its trajectory under ℓ_μ^k remains in $J_1(N_1)$ and never enters $J_1(N_2)$ by recurrence. Hence the closest point of N_3 is bigger than $\rho(N_1) > \rho(N_3) > \rho(N_2)$. □

There is an immediate important corollary of the proposition above.

Corollary 4. *For every repelling node N, there are only finitely many nodes N' such that $N' > N$.*

Proposition 6 (Repelling nodes). *Every repelling node of ℓ_μ is either a flip periodic orbit or a Cantor set.*

Proof. Let $N_1, N_2, \dots$ be the set of nodes of ℓ_μ ordered so that $\rho(N_i) > \rho(N_j)$ if $i < j$. Then, N_i is the set of chain-recurrent points in $J^{int}(N_i) \setminus J^{int}(N_{i+1})$. Denote by $\bar{\ell}$ the power $|\mathcal{T}(N_i)|$ of ℓ_μ. We can always reduce the problem of the structure of the set N_{i+1} to the problem of the structure of the set of points of the single interval $J_1(N_i)$ not falling, under $\bar{\ell}$, on the cyclic trapping region $\mathcal{S} = \{J_1, \dots, J_k\}$ of $J_1(N_i)$ of period $k = |\mathcal{T}(N_{i+1})|/|\mathcal{T}(N_i)|$. Note that $J_1 = J_1(N_{i+1})$.

Assume first that $\mathcal{S}$ is regular. Then, in particular:

1. $J_i \cap J_j = \emptyset$ for $i \neq j$;

2. for all $i \neq 1$, the set $\bar{\ell}^{-1}(J_{i+1})$, where $k+1$ is meant mod k, is the disjoint union of J_i and a second interval $\hat{J}_i$, on each of which ℓ_μ restricts to a diffeomorphism with J_i;
3. $\bar{\ell}^{-1}(J_2) = J_1$. In this case every point of J_1 is covered by two points of J_2 except for the critical point c.

Now, take any two intervals A and B that are connected components of, respectively, $\bar{\ell}^{-p}(J_i)$ and $\bar{\ell}^{-q}(J_j)$. Assume, to avoid trivial cases, that neither A nor B are equal to J_1. Then, after enough iterations of $\bar{\ell}$, say r, $\bar{\ell}^r(A)$ and $\bar{\ell}^r(B)$ will be subsets, respectively, of two intervals J_{i_A} and J_{i_B} and at least either $\bar{\ell}^r(A)$ or $\bar{\ell}^r(B)$ will be actually equal to that interval.

If $i_A \neq i_B$, then $\bar{\ell}^r(A) \cap \bar{\ell}^r(B) = \emptyset$ and therefore also $A \cap B = \emptyset$. If $i_A = i_B = i$, it means that A and B are backward iterates of the same J_i. In that case, after applying enough times $\bar{\ell}$, we will have that $J_i \cap \bar{\ell}^{rk}(J_i) \neq \emptyset$ for some positive integer r. The only non-trivial case is when this intersection is a single point. In this case, the common point must be the periodic endpoint, but this can happen only if $\mathcal{S}$ is a flip cyclic trapping region, against the hypothesis.

Ultimately, therefore, the set of points of $J_1(N_i)$ that never fall in $J^{int}(\mathcal{S})$ is the complement of a countable dense set of open intervals whose closures are pairwise disjoint. Hence, it is a Cantor set and the action of $\bar{\ell}$ on it is a subshift of finite type. The node N_{i+1} is a closed invariant subset of a finite union of such Cantor sets, and therefore is itself a Cantor set.

Assume now that $\mathcal{S}$ is a flip cyclic trapping region. Then $\mathcal{S} = \{J_1, J_2\}$, with $J_1 = J_1(N_{i+1})$. Hence, $\mathcal{S}$ is as in Fig. 9, namely $J_1 = [q_1, p_1]$ and $J_2 = [p_1, q_2]$, where $p_1 = p_1(N_{i+1})$ is fixed for $\bar{\ell}$. Then $\bar{\ell}^{-1}(J_1)$ is the disjoint union of J_2 and the interval $A = [\hat{q}_1, q_1]$, where $\hat{q}_1$ is the counterimage of q_1 at the left of c, while $\bar{\ell}^{-1}(J_2) = J_1$. The two counterimages of A are the intervals $A_1 = [\hat{\hat{q}}_1, \hat{q}_1]$ and $A_2 = [\bar{q}_1, \bar{\bar{q}}_1]$, where $\hat{\hat{q}}_1$ is the counterimage of $\hat{q}_1$ at the left of c, $\bar{\bar{q}}_1$ the one at the right of c and $\bar{q}_1 = q_2$ is the counterimage of q_1 at the right of c. Similarly, at every new recursion step, two new intervals arise, one at the left of c and having an endpoint in common with the interval at the left of c obtained at the previous recursion level and one at the right with similar properties.

Ultimately, then, the set of points of $J_1(N_i)$ that do not fall eventually into $J^{int}(N_{i+1})$ under $\bar{\ell}$ is the union of the fixed point $p_1(N_i)$ together with all of its counterimages under $\bar{\ell}$. These counterimages can be sorted into two subsequences which converge monotonically to the endpoints of $J_1(N_i)$. Hence, in this case N_{i+1} consists exactly in the flip periodic orbit through $p_1(N_{i+1})$. □

The next proposition asserts that each attracting node A of ℓ_μ is one of the following five types.

(A_1) An attracting periodic orbit.
(A_2) A trapping region; here the attractor is a finite collection of intervals.
(A_3) An attracting Cantor set; this is the attracting node when the number of nodes is infinite;
(A_4) A repelling Cantor set containing a 1-sided attracting periodic orbit. This occurs precisely for those μ for which there is a periodic orbit that is at the beginning of a window, where there is an attractor-repellor periodic orbit bifurcation. That periodic orbit is a one-sided attractor and it is in a Cantor set. Fig. 7 gives an example: at μ_{70} there is a period-3 attractor-repellor bifurcation and p_1 is one of the three points of the attractor-repellor orbit,

the one closest to the critical point. Here there are two nodes: 0 and the red Cantor set, to which the orbit belongs to.

(A_5) A trapping region which strictly contains an attracting cyclic trapping region, a repelling Cantor set and part of the basin of attraction. This occurs precisely for those μ at the end of a window, where c eventually maps onto the periodic orbit on the edge of a cyclic trapping region. Fig. 7 gives an example: at μ_{7e} there is a crisis, the critical point eventually maps onto p_1. The line segment from q_1 to p_1 is J_1. The node, however, is the whole interval from q_3 to q_2, which includes J^{int}. Notice that, at such crisis values, $\ell_\mu(J_1) = J_2$, namely $q_2 = \ell_\mu(c)$. In particular, $\ell_\mu^6(c) = p_1$.

Proposition 7 (**Attracting nodes**). *The attracting node A of ℓ_μ is one of the above five types.*

Proof. The first three cases are those when an attracting node coincides with the attractor. We have case (1) for almost all $\mu \in \mathcal{A}_P$, for instance for all $\mu \in (0, \mu_{FM})$. We have case (2) for almost all $\mu \in \mathcal{A}_C$, for instance for $\mu = 2(1 + (19 + 3\sqrt{33})^{1/3} + (19 - 3\sqrt{33})^{1/3})/3$. At this parameter value, the critical point falls on the unstable fixed point in $(0, 1)$ at its third iterate. This is the first μ for which the chaotic attractor is a single interval. We have case (3) for all $\mu \in \mathcal{A}_{AP}$.

Unlike the case of repelling nodes, though, in which case every two nodes have different distance from c and so cannot ever merge, an attracting node can, in degenerate cases, merge with a repelling one.

When an attracting periodic orbit merges with a repelling one, we have an orbit that is attracting on one side and repelling on the other. This happens at every bifurcation point of a cascade. The node, though, in this case is still of type (1).

When an attracting periodic orbit merges with a repelling Cantor set, we have a Cantor set whose points are all repelling except for a single periodic orbit, which is a 1-sided attractor. This is type (4). We get this kind of node at the first point of each window, e.g. at $\mu = 1 + \sqrt{8}$ (see Fig. 2).

When an attracting trapping region merges with a repelling periodic orbit, the trapping region becomes a cyclic trapping region. We have this at $\mu = 4$. The repelling node in this case is still of type (2).

At the end of each window, the attractor is a trapping region with a periodic orbit in common with a repelling Cantor set. In this case the attractor is a cyclic trapping region and the node is equal to a trapping region which contains, besides the attractor, the Cantor set with the orbit in common with the attractor and part of the basin of attraction. We get this, for instance, at $\mu = 3.8568...$ (see Fig. 2). □

Definition 3.14. We say that a point x in a node N is **accessible** [2, 16, 1] if there is a closed interval K with x as endpoint such that $K \cap N = \{x\}$. We call K an **access interval** of the node. A periodic orbit is accessible if all of its points are accessible.

Notice that each periodic orbit is in some node. A node can either consist in a single periodic orbit or contain infinitely many.

Theorem 3.15. *Let N be a node of ℓ_μ with $\rho(N) > 0$. Then N has a unique accessible periodic orbit in it. This accessible orbit is orbit(N) and $J_1(N)$ is an access interval of N.*

Proof. The claim is trivial when the node is a periodic orbit, so we assume that N is a Cantor set. By the same arguments used in the proof of Prop. 6, for each pair

of points $x, y \in N$, $x < y$, between which lie no other point of N, there is some integer r such that

$$\ell_\mu^r((x,y)) = \mathrm{int}(J_1(N)).$$

In particular, x and y are preperiodic and fall eventually in orbit(N). One of them might be periodic. □

Edges. The following proposition is the last non-trivial step we need in order to prove that the graph is a tower:

Proposition 8. *If N and N' are nodes and $N > N'$, then there is an edge from N to N'.*

Proof. By construction, the node N has no common point with $J^{int}(\mathcal{T}_N)$. Since N' is closer to c than N, on the contrary, at least one of its points lies in the interior of $J_1(N)$ and therefore the whole N' lies in $J^{int}(\mathcal{T}_N)$.

By Prop. 3, each point $x \in N'$ is downstream from $p_1(N)$. Since $p_1(N)$ is periodic, for every $\varepsilon > 0$ there is a trajectory t_ε starting in $(p_1, p_1 + \varepsilon)$ and falling eventually on x. Since p_1 is repelling, for each point y close enough to p_1 there is a trajectory t passing through y with $\alpha(t) = N$. In other words, there are trajectories backward asymptotic to N from any node inside $\mathcal{T}_N$, namely there is an edge from N to any node in $J^{int}(N)$.

□

Now, the main result of our article comes immediately from Prop. 2 and Prop. 8.

Theorem 3.16. *The graph of ℓ_μ is a tower. The tower is infinite if and only if $\mu \in \mathcal{A}_{AP}$.*

Several examples of towers are shown in Figs. 1 and 2. The white node on top is the node $N_0 = \{0\}$. Its trapping region is the single interval $J_1 = [0, 1]$. Each green node is a repelling periodic orbit, the red and blue nodes are repelling Cantor sets shown with the same color in figure. The black node is the attracting node. Notice that, in all towers in the interior of the period-3 window, the second node N_1 of the tower is the red Cantor set of all chain-recurrent points not falling eventually in $J^{int}(N_1)$. In general, the number of repelling Cantor set nodes in the graph of ℓ_μ is equal to the number of its regular repelling trapping regions, that is, the number of nested windows at μ.

Assigning weights to the edges of the graph. As shown in Prop. 5, the edge between N_i to N_{i+1} has a weight associated to it equal to $w_i = |\mathcal{T}(N_{i+1})|/|\mathcal{T}(N_i)|$. Recall that, in the logistic map, there are windows of any period $k \geq 3$ and the structure of the bifurcation diagram is closely repeated in every subwindow. Hence, given any finite or infinite sequence of strictly increasing integers s_n starting with $s_1 = 1$ and such that $s_n = w_n s_{n+1}$, there is a μ in parameter space such that there is a node N_n for each n with $s_n = |\mathcal{T}(N_n)|$. Furthermore, if $w_n = 2$, then $\mathcal{T}(N_n)$ is a flip trapping region and N_n is a flip periodic orbit. If, instead, $w_n \neq 2$, then $\mathcal{T}(N_n)$ is a regular trapping region and N_n it is either a Cantor set or the attractor.

Spectral Theorem. Next statement collects all most important results we achieved into a "chain-recurrent" version of the Spectral Theorem.

Theorem 3.17 (Chain-Recurrent Spectral Theorem)**.** *Let $\mu \in (1,4)$ and denote by $N_0, N_1, \ldots, N_p$, where p is possibly infinite, the nodes of ℓ_μ sorted so that $N_i > N_j$ if $i < j$. Then:*

1. *the cyclic trapping regions $\mathcal{T}_j = \mathcal{T}(N_j)$, $0 \le j < p$, are nested in each other:*
$$cl(J^{int}(\mathcal{T}_j)) \subset J^{int}(\mathcal{T}_{j-1}),\ 1 \le j < p.$$
2. *Every point in $J^{int}(\mathcal{T}_j)$ falls eventually under ℓ_μ either onto N_j or onto $J^{int}(\mathcal{T}_{j+1})$ for all $0 \le j < p$. (Prop. 5)*
3. *$\mathcal{R}_{\ell_\mu}$ writes uniquely as the disjoint union of its nodes $N_0, N_1, \ldots, N_p$.*
4. *$N_0 = \{0\}$.*
5. *Each N_j, $1 \le j < p$, is either a Cantor set or a periodic flip orbit (Prop. 6). If it is a Cantor set, the action of ℓ_μ on it is a subshift of finite type with a dense orbit* [37].
6. *Each N_j, $0 \le j < p$, is repelling and hyperbolic* [37].
7. *N_p is the unique attracting node of ℓ_μ* [17] *and it is one of the five types $A_1, \ldots, A_5$. (Prop. 7)*
8. *N_p is hyperbolic except when μ is at the endpoints of a window* [37] *(cases A_4 and A_5).*
9. *In each neighborhood of N_i, for each $j \ge i$, there are points falling eventually into N_j. (Prop 8)*
10. *When $p = \infty$, the attracting node N_∞ is a Cantor set on which ℓ_μ acts as an adding machine* [37].

Acknowledgments. The authors are grateful to Todd Drumm and Michael Jakobson for helpful conversations on the paper's topic. All calculations to produce the pictures in the present article were performed on the HPCC of the College of Arts and Sciences at Howard University with C++ code wrote by the first author.

REFERENCES

[1] K. Alligood and J. Yorke, Accessible saddles on fractal basin boundaries, *Ergodic Theory and Dynamical Systems*, **12** (1992), 377–400.
[2] G. Birkhoff, Sur quelques courbes fermées remarquables, *Bulletin de la Société mathématique de France*, **60** (1932), 1–26.
[3] A. Blokh, The "spectral" decomposition for one-dimensional maps, in *Dynamics Reported*, Springer, 1995, 1–59.
[4] A. Blokh and M. Lyubich, Measurable dynamics of S-unimodal maps of the interval, in *Annales Scientifiques de l'Ecole Normale Supérieure*, **24** (1991), 545–573.
[5] R. Bowen, ω-limit sets for axiom A diffeomorphisms, *Journal of Differential Equations*, **18** (1975), 333–339.
[6] J. Buescu, *Exotic Attractors: From Liapunov Stability to Riddled Basins*, 153, Birkhäuser, 2012.
[7] X. Chen and P. Polácik, Gradient-like structure and Morse decompositions for time-periodic one-dimensional parabolic equations, *Journal of Dynamics and Differential Equations*, **7** (1995), 73–107.
[8] C. Conley, On a generalization of the morse index, in *Ordinary Differential Equations*, Elsevier, 1972, 27–33.
[9] C. Conley, *Isolated Invariant Sets and the Morse Index*, 38, American Mathematical Soc., 1978.
[10] R. De Leo and J. Yorke, Infinite towers in the graph of a dynamical system, *Nonlinear Dynamics* (to appear), *arXiv E-prints*, arXiv:2101.00306.
[11] W. de Melo and S. van Strien, A structure theorem in one dimensional dynamics, *Annals of Mathematics*, **129** (1989), 519–546.

[12] W. de Melo and S. van Strien, *One-Dimensional Dynamics*, 25, Springer Science & Business Media, 1993. Available from: URL http://www2.imperial.ac.uk/~svanstri/Files/demelo-strien.pdf.
[13] M. Feigenbaum, Quantitative universality for a class of nonlinear transformations, *Journal of Statistical Physics*, **19** (1978), 25–52.
[14] J. Graczyk and G. Swiatek, Generic hyperbolicity in the logistic family, *Annals of Mathematics*, 1–52.
[15] C. Grebogi, E. Ott and J. Yorke, Chaotic attractors in crisis, *Physical Review Letters*, **48** (1982), 1507.
[16] C. Grebogi, E. Ott and J. Yorke, Basin boundary metamorphoses: Changes in accessible boundary orbits, *Nuclear Physics B-Proceedings Supplements*, **2** (1987), 281–300.
[17] J. Guckenheimer, Sensitive dependence to initial conditions for one dimensional maps, *Communications in Mathematical Physics*, **70** (1979), 133–160.
[18] J. Hale, L. Magalhães and W. Oliva, *Dynamics in Infinite Dimensions*, 47, Springer Science & Business Media, 2006.
[19] M. Hirsch, H. Smith and X. Zhao, Chain transitivity, attractivity, and strong repellors for semidynamical systems, *Journal of Dynamics and Differential Equations*, **13** (2001), 107–131.
[20] P. Holmes and D. Whitley, Bifurcations of one-and two-dimensional maps, *Philosophical Transactions of the Royal Society of London. Series A, Mathematical and Physical Sciences*, **311** (1984), 43–102.
[21] M. Hurley, Chain recurrence and attraction in non-compact spaces, *Ergodic Theory and Dynamical Systems*, **11** (1991), 709–729.
[22] M. Jakobson, Absolutely continuous invariant measures for one-parameter families of one-dimensional maps, *Communications in Mathematical Physics*, **81** (1981), 39–88.
[23] L. Jonker and D. Rand, Bifurcations in one dimension, *Inventiones Mathematicae*, **62** (1980), 347–365.
[24] M. Lyubich, Dynamics of quadratic polynomials, I–II, *Acta Mathematica*, **178** (1997), 185–297.
[25] M. Lyubich, Almost every real quadratic map is either regular or stochastic, *Annals of Mathematics*, 1–78.
[26] J. Mallet-Paret, Morse decompositions for delay-differential equations, *Journal of Differential Equations*, **72** (1988), 270–315.
[27] J. Milnor, On the concept of attractor, in *The Theory of Chaotic Attractors*, Springer, 1985, 243–264.
[28] D. Norton, The Conley decomposition theorem for maps: a metric approach, *Rikkyo Daigaku Sugaku Zasshi*, **44** (1995), 151–173.
[29] D. Norton, The fundamental theorem of dynamical systems, *Commentationes Mathematicae Universitatis Carolinae*, **36** (1995), 585–597.
[30] M. Patrão, Morse decomposition of semiflows on topological spaces, *Journal of Dynamics and Differential Equations*, **19** (2007), 181–198.
[31] K. Rybakowski, *The Homotopy Index and Partial Differential Equations*, Springer, 1987.
[32] A. Sharkovsky, S. Kolyada, A. Sivak and V. Fedorenko, *Dynamics of One-Dimensional Maps*, 407, Springer Science & Business Media, 1997.
[33] D. Singer, Stable orbits and bifurcation of maps of the interval, *SIAM Journal on Applied Mathematics*, **35** (1978), 260–267.
[34] S. Smale, On gradient dynamical systems, *Annals of Mathematics*, 199–206.
[35] S. Smale, Differentiable dynamical systems, *Bulletin of the American mathematical Society*, **73** (1967), 747–817.
[36] S. Smale and R. Williams, The qualitative analysis of a difference equation of population growth, *Journal of Mathematical Biology*, **3** (1976), 1–4.
[37] S. van Strien, On the bifurcations creating horseshoes, in *Dynamical Systems and Turbulence, Warwick 1980*, Springer, 1981, 316–351.
[38] F. Wilson and J. Yorke, Lyapunov functions and isolating blocks, *Journal of Differential Equations*, **13** (1973), 106–123.

Received for publication November 2020.

E-mail address: roberto.deleo@howard.edu
E-mail address: yorke@umd.edu